

Nuclear Hartree-Fock calculations with splines

A.S. Umar,⁽¹⁾ M.R. Strayer,⁽²⁾ J.-S. Wu,⁽²⁾ D.J. Dean,^(1,2) and M.C. Güçlü⁽¹⁾

Center for Computationally Intensive Physics, Physics Division, Oak Ridge National Laboratory, Oak Ridge, Tennessee 37831

⁽¹⁾*Vanderbilt University, Department of Physics and Astronomy, Nashville, Tennessee 37235*

⁽²⁾*Physics Division, Oak Ridge National Laboratory, Oak Ridge, Tennessee 37831*

(Received 6 May 1991)

We present the numerical details for performing static Hartree-Fock and time-dependent Hartree-Fock calculations using a spline collocation method. Calculations are performed on a three-dimensional Cartesian lattice without any symmetry assumptions and quantal degeneracies. The three-dimensional Hartree-Fock calculations are compared with the solutions of the corresponding radial equations. The results demonstrate an unprecedented accuracy for relatively coarse meshes. We also present a zero impact parameter, time-dependent Hartree-Fock calculation for the $^{16}\text{O}+^{16}\text{O}$ system.

I. INTRODUCTION

The mean-field formalism has been a successful approximation to the nuclear many-body problem for reproducing the principal properties of nuclei throughout the periodic table. The details of these calculations suggest that the Pauli principle plays an important role in simultaneously building up a mean field and suppressing the strong N - N interaction terms. The time-dependent mean-field formalism has proven to be a valuable tool for studying a variety of nuclear phenomena, e.g., fusion, fission, deep-inelastic scattering, and nuclear molecular resonances. A comprehensive review of the previous applications can be found in Refs. [1–4].

From the numerical standpoint, new techniques have been developed to handle the solution of the Hartree-Fock equations on a space-time lattice. In particular, equations of motion were obtained via the variation of the lattice representations of the constants of the motion, such as the total energy [5–8]. In this variation after discretization approach, resulting equations exactly preserve the constants of the motion. The lattice techniques are important because the alternative basis expansion approach requires the optimization of basis set parameters due to the finite cutoff in the number of basis states. This procedure becomes very inefficient for large-scale calculation of, say, multidimensional energy surfaces using realistic density-dependent interactions. Due to their extensive computational requirements most numerical calculations have employed low-order, finite-difference discretization techniques with accuracies appropriate for studying the gross features of heavy-ion collisions. For example, time-dependent Hartree-Fock (TDHF) calculations have been performed with imposed spin-symmetry, no spin-orbit interaction, and using an axially symmetric geometry. Recently, we have shown that the relaxation of the spin-symmetry is an important consideration for the dissipation of the relative kinetic energy in low-energy heavy-ion collisions [5, 9–11].

With the advent of new supercomputer technologies, it has become feasible to carry out more extensive nuclear structure and reaction studies without resorting to the symmetry assumptions employed in the earlier applications. Typical calculations would include the study of highly excited deformed systems, e.g., multidimensional energy surfaces and superdeformations, and nuclear fission. Calculation of nuclear properties away from the ground state are important in establishing the detailed form and parametrization of the effective interaction employed in these calculations. Most realistic effective interactions, such as the Skyrme (SkM*) force, are fitted to reproduce the ground-state properties of a few spherical nuclei. An exception is the SkM* force which also approximately reproduces the one-dimensional fission barrier of ^{240}Pu [12].

In order to be able to perform such calculations and to obtain a more detailed comparison with data it is necessary to exploit higher-order interpolation techniques. This is due to the fact that precise nuclear structure studies would require overall accuracies which are a fraction of a MeV. Considering the fact that such small numbers arise from the cancellation of large attractive and repulsive parts, the calculational accuracy of each part should be better than 0.1%. Along these lines a series of Hartree-Fock (HF) and HF-BCS calculations have been carried out for medium-heavy nuclei using seventh and ninth-order finite-difference discretization of the differential operators [13–17]. These calculations were performed on a three-dimensional Cartesian lattice with imposed parity and z -signature symmetries [13, 14]. Discretization of the energy functional on a spline collocation lattice provides a highly accurate alternative to the finite-difference method. One significant advantage of this technique is that in comparison to the finite-difference method the same level of accuracy can be attained with a smaller number of lattice points. The structure of the resulting lattice representation is highly suited for vector and parallel supercomputers, and the method allows a highly

modular programming where the order of the splines can be defined as an input parameter. Further details of the spline collocation method are published elsewhere [18, 19].

In this paper we present three-dimensional, HF and TDHF calculations with no imposed symmetries, using the spline collocation method. In Sec. II we briefly introduce the basic HF and TDHF equations using the Skyrme interaction. In Sec. III we obtain a collocation-lattice representation of the HF equations. This section also contains the methods for solving the resulting systems of equations. Section IV presents the results for static and dynamic calculations, and in Sec. V we present a discussion of the results.

II. FORMALISM

In this section we will outline the static and dynamic Hartree-Fock equations using the Skyrme effective interaction.

A. Formal equations

Given a many-body Hamiltonian containing two- and three-body interactions

$$H = \sum_i^N t_i + \sum_{i<j}^N v_{ij} + \sum_{i<j<k}^N v_{ijk}, \quad (1)$$

the time-dependent action S can be constructed as [20]

$$S = \int_{t_1}^{t_2} dt \langle \Phi(t) | H - i\hbar \partial_t | \Phi(t) \rangle. \quad (2)$$

Here, $\Phi(t)$ denotes the time dependent, many-body wave function which, for a system of fermions, is commonly approximated by a Slater determinant. Variation of the action yields the most probable time-dependent path between the points t_1 and t_2 in the multidimensional space-time phase space

$$\delta S = 0 \rightarrow \Phi(t) = \Phi_0(t). \quad (3)$$

In practice $\Phi_0(t)$ is chosen to be a Slater determinant

$$\Phi_0(t) = \frac{1}{\sqrt{N!}} \det |\phi_\lambda(\mathbf{r}, t)|, \quad (4)$$

where $\phi_\lambda(\mathbf{r}, t)$ are the single-particle states with quantum numbers λ . If the variation in Eq. (3) is performed with respect to the single-particle states ϕ_λ^* , we obtain a set of coupled, nonlinear, self-consistent initial-value equations for the single-particle states

$$h(\{\phi_\mu\}) \phi_\lambda = i\hbar \dot{\phi}_\lambda, \quad \lambda = 1, \dots, N. \quad (5)$$

These are the fully microscopic time-dependent Hartree-Fock equations which preserve the major conservation laws such as the particle number, total energy, etc.

Static equations can be obtained from Eq. (5) by taking out a trivial phase from the single-particle states

$$h(\{\chi_\mu\}) \chi_\lambda = \epsilon_\lambda \chi_\lambda, \quad (6)$$

$$\phi_\lambda(\mathbf{r}, t) = e^{-i\epsilon_\lambda t/\hbar} \chi_\lambda(\mathbf{r}).$$

For time-dependent calculations the initial single-particle states can be constructed from the static solutions by multiplying them with an appropriate phase factor (or boost)

$$\phi_\lambda(t=0) = e^{i\mathbf{k}\cdot\mathbf{r}} \chi_\lambda(\mathbf{r}). \quad (7)$$

This corresponds to multiplying the static Slater determinant by a plane wave $\exp(i\mathbf{k}\cdot\mathbf{R})$, where $\mathbf{R} = \sum_i \mathbf{r}_i$ and leads to a translating solution due to the Galilean invariance of the equations of motion.

B. Skyrme potential

As the effective two-body interaction, we employed the Skyrme potential with a generalized density-dependent term [12, 21–24]

$$\begin{aligned} v^{(2)}(\mathbf{r}_1, \mathbf{r}_2) = & t_0(1 + x_0 P_\sigma) \delta(\mathbf{r}_1 - \mathbf{r}_2) + \frac{t_1}{2} [\delta(\mathbf{r}_1 - \mathbf{r}_2) \mathbf{k}^2 + k'^2 \delta(\mathbf{r}_1 - \mathbf{r}_2)] + t_2 \mathbf{k}' \cdot \delta(\mathbf{r}_1 - \mathbf{r}_2) \mathbf{k} \\ & + \frac{t_3}{6} (1 + x_3 P_\sigma) \rho^\alpha(\mathbf{R}) \delta(\mathbf{r}_1 - \mathbf{r}_2) + it_4 (\boldsymbol{\sigma}_1 + \boldsymbol{\sigma}_2) \cdot \mathbf{k}' \times \delta(\mathbf{r}_1 - \mathbf{r}_2) \mathbf{k}, \end{aligned} \quad (8)$$

where

$$\mathbf{k} = \frac{\nabla_1 - \nabla_2}{2i}, \quad \mathbf{k}' = \mathbf{k}^\dagger, \quad P_\sigma = \frac{1 + \boldsymbol{\sigma}_1 \cdot \boldsymbol{\sigma}_2}{2}. \quad (9)$$

In Eq. (8), the term proportional to t_3 is a density-dependent term which has the same expectation value as a local three-body interaction for $\alpha = x_3 = 1$. The term with coefficient t_4 is the spin-orbit interaction used in earlier calculations.

The expectation value of H with the above interaction can be written in terms of the energy density $\mathcal{H}(\mathbf{r})$ as [21, 22]

$$E = \langle \Phi | H | \Phi \rangle = \int d^3r \mathcal{H}(\mathbf{r}). \quad (10)$$

The energy density is commonly decomposed into various groups as given below

$$\mathcal{H} = \mathcal{H}_0 + \mathcal{H}_{LS} + \mathcal{H}_C + \mathcal{H}_Y, \quad (11)$$

$$\begin{aligned} \mathcal{H}_0 &= \frac{\hbar^2}{2m} \tau + \frac{t_0}{2} \left(1 + \frac{x_0}{2}\right) \rho^2 - \frac{t_0}{2} \left(\frac{1}{2} + x_0\right) \sum_q \rho_q^2 + \frac{t_3}{12} \left(1 + \frac{x_3}{2}\right) \rho^{\alpha+2} - \frac{t_3}{12} \left(\frac{1}{2} + x_3\right) \rho^\alpha \sum_q \rho_q^2 \\ &\quad + \frac{1}{4}(t_1 + t_2)[\rho\tau - j^2] - \frac{1}{8}(t_1 - t_2) \sum_q (\rho_q \tau_q - j_q^2), \\ \mathcal{H}_{LS} &= -\frac{t_4}{2} [\rho \nabla \cdot \mathbf{J} + \sum_q \rho_q (\nabla \cdot \mathbf{J}_q)], \end{aligned}$$

$$\mathcal{H}_C = \frac{1}{2} e^2 \int d^3 r' \rho_p(\mathbf{r}) \frac{1}{|\mathbf{r} - \mathbf{r}'|} \rho_p(\mathbf{r}') - \frac{3}{4} e^2 \left(\frac{3}{\pi}\right)^{\frac{1}{3}} [\rho_p(\mathbf{r})]^{\frac{4}{3}}, \quad (12)$$

and

$$\mathcal{H}_Y = \begin{cases} \int d^3 r' \frac{\exp(-|\mathbf{r} - \mathbf{r}'|/a)}{|\mathbf{r} - \mathbf{r}'|/a} \left[\frac{V_U}{2} \rho(\mathbf{r}) \rho(\mathbf{r}') + \frac{V_L - V_U}{2} \sum_q \rho_q(\mathbf{r}) \rho_q(\mathbf{r}') \right] \\ \text{or} \\ \frac{1}{16} (t_2 - 3t_1) \rho \nabla^2 \rho + \frac{1}{32} (t_2 + 3t_1) \sum_q \rho_q \nabla^2 \rho_q. \end{cases} \quad (13)$$

The finite-range form of the \mathcal{H}_Y term [7] is usually preferred in dynamical calculations because of its numerical stability and better surface properties. We also note that the Coulomb term \mathcal{H}_C contains a Slater exchange contribution in addition to the direct term. Various quantities used in the energy density are written in terms of the spin-up and spin-down components of the single-particle states

$$\phi_\lambda = \begin{pmatrix} \psi_\lambda^+ \\ \psi_\lambda^- \end{pmatrix}, \quad (14)$$

as

$$\begin{aligned} \rho_q(\mathbf{r}) &= \sum_{\lambda \in q} n_\lambda \{ |\psi_\lambda^+(\mathbf{r})|^2 + |\psi_\lambda^-(\mathbf{r})|^2 \}, \\ \tau_q(\mathbf{r}) &= \sum_{\lambda \in q} n_\lambda \{ |\nabla \psi_\lambda^+(\mathbf{r})|^2 + |\nabla \psi_\lambda^-(\mathbf{r})|^2 \}, \\ \mathbf{j}_q(\mathbf{r}) &= \sum_{\lambda \in q} n_\lambda \text{Im} \left[\psi_\lambda^{+*}(\mathbf{r}) \nabla \psi_\lambda^+(\mathbf{r}) + \psi_\lambda^{-*}(\mathbf{r}) \nabla \psi_\lambda^-(\mathbf{r}) \right], \\ \mathbf{J}_q(\mathbf{r}) &= -i \sum_{\substack{\lambda \in q \\ \mu \mu' = \pm}} n_\lambda \psi_\lambda^{\mu*}(\mathbf{r}) (\nabla \times \sigma) \psi_\lambda^{\mu'}(\mathbf{r}'). \end{aligned}$$

Here, the subscript $q = n, p$ denotes the isospin quantum number and the total density is simply $\rho = \rho_n + \rho_p$ (same for all other quantities as well). The quantities n_λ are the occupation numbers for the state λ .

C. Hartree-Fock Hamiltonian

Using the Skyrme effective interaction and the one-body kinetic energy term, the Hartree-Fock Hamiltonian can be written as

$$\begin{aligned} h_q &= -\nabla \cdot \frac{\hbar^2}{2m_q(\mathbf{r})} \nabla + U_q + U_Y + U_C \\ &\quad + \frac{1}{2i} (\nabla \cdot \mathbf{I}_q + \mathbf{I}_q \cdot \nabla) - i \mathbf{B}_q \cdot (\nabla \times \sigma). \end{aligned} \quad (15)$$

Various terms in the above expression are given by

$$\begin{aligned} \frac{\hbar^2}{2m_q(\mathbf{r})} &= \frac{\hbar^2}{2m} + \frac{1}{4}(t_1 + t_2)\rho + \frac{1}{8}(t_2 - t_1)\rho_q, \\ \mathbf{I}_q &= -\frac{1}{2}(t_1 + t_2)\mathbf{j} - \frac{1}{4}(t_2 - t_1)\mathbf{j}_q, \\ \mathbf{B}_q &= -\frac{1}{8}(t_2 - t_1)\mathbf{J}_q + \frac{t_4}{2}\nabla(\rho + \rho_q), \end{aligned} \quad (16)$$

and

$$\begin{aligned} U_q &= t_0 \left[\left(1 + \frac{x_0}{2}\right) \rho - \left(\frac{1}{2} + x_0\right) \rho_q \right] + \frac{1}{4}(t_1 + t_2)\tau - \frac{1}{8}(t_1 - t_2)\tau_q \\ &\quad + \frac{t_3}{12} \left(1 + \frac{x_3}{2}\right) [\alpha + 2]\rho^{\alpha+1} - \frac{t_3}{12} \left(\frac{1}{2} + x_3\right) \left(\alpha \rho^{\alpha-1} \sum_q \rho_q^2 + 2\rho^\alpha \rho_q \right) - \frac{t_4}{2} [\nabla \cdot \mathbf{J} + \nabla \cdot \mathbf{J}_q]. \end{aligned} \quad (17)$$

The Yukawa and Coulomb contributions are

$$U_Y = \begin{cases} \int d^3r' \frac{\exp(-|\mathbf{r} - \mathbf{r}'|/a)}{|\mathbf{r} - \mathbf{r}'|/a} [V_U \rho(\mathbf{r}') + (V_L - V_U) \rho_q(\mathbf{r}')] \\ \text{or} \\ \frac{1}{8}(t_2 - 3t_1) \nabla^2 \rho + \frac{1}{16}(t_2 + 3t_1) \nabla^2 \rho_q, \end{cases} \quad (18)$$

$$U_C = e^2 \int d^3r' \frac{\rho_p(\mathbf{r}')}{|\mathbf{r} - \mathbf{r}'|} - e^2 \left(\frac{3}{\pi}\right)^{\frac{1}{3}} [\rho_p(\mathbf{r})]^{\frac{1}{3}}. \quad (19)$$

The first term in the definition of \mathbf{B}_q is neglected in practical calculations. Table I lists the parameter values for various forms of the Skyrme force used in our calculations.

III. SPLINE IMPLEMENTATION

Currently, most HF and TDHF calculations are performed using low-order finite difference lattice techniques. It is desirable to investigate higher-order interpolation methods which result in the improvement of the overall accuracy and reduction in the total number of lattice points. The lattice solution of differential equations on a discretized mesh of independent variables may be viewed to proceed in two steps: (1) Obtain a discrete representation of the functions and operators on the lattice. (2) Solve the resulting lattice equations using iterative techniques. Step (1) is an interpolation problem for which we could take advantage of the techniques developed using the spline functions [25, 18]. The use of the spline collocation method leads to a matrix-vector representation on the collocation lattice with a metric describing the transformation properties of the collocation lattice.

TABLE I. Parameter values for various parametrizations of the Skyrme force used in our calculations. The BKN force is from Ref. [27], the SkM* force from Ref. [12]. The subscript Y indicates that the $\nabla^2 \rho$ terms are replaced by the Yukawa form.

Force	BKN	SkM*	(SkM*) _Y
t_0 (MeV fm ³)	-497.726	-2645.0	-1784.692
t_1 (MeV fm ⁵)	0.0	410.0	410.0
t_2 (MeV fm ⁵)	0.0	-135.0	-135.0
t_3 (MeV fm ⁶)	17270.0	15595.0	15595.0
t_4 (MeV fm ⁵)	0.0	130.0	130.0
x_0	1.0	0.09	0.19302
x_3	1.0	0.0	0.0
α	1.0	1/6	1/6
V_U (MeV)	-363.044		-660.7470
V_L (MeV)	-363.044		-395.7221
a (fm)	0.45979		0.45979

A. Splines

Given a set of points or *knots* denoted by the set $\{x_i\}$, a spline function of order M , denoted by B_i^M , is constructed from continuous piecewise polynomials of order $M - 1$. These splines have continuous derivatives up to a $(M - 2)$ nd derivative and a discontinuous $(M - 1)$ st derivative. We only consider odd-order splines or even-order polynomials for reasons related to the choice of the collocation points. The i th spline is nonzero only in the interval (x_i, x_{i+M}) . This property is commonly referred to as limited support. The knots are the points where polynomials making up the spline join. In the interval containing the tail region, the splines fall off very rapidly to zero. The explicit construction of the splines is explained elsewhere [18]. We can also construct exact derivatives of splines provided the derivative order does not exceed $M - 1$.

A continuous function $f(x)$, defined in the interval (x_{\min}, x_{\max}) , can be expanded in terms of spline functions as

$$f(x) = \sum_i B_i^M(x) c^i, \quad (20)$$

where quantities c^i denote the expansion coefficients. We can solve for the expansion coefficients in terms of a given, or to be determined, set of function values evaluated at a set of data points more commonly known as *collocation points*. There are a number of ways to choose collocation points [18, 25]; however, for odd-order splines a simple choice is to place one collocation point at the center of each knot interval within the physical boundaries

$$x_\alpha = \frac{x_{\alpha+M-1} + x_{\alpha+M}}{2}, \quad \alpha = 1, \dots, N. \quad (21)$$

Here, $x_M = x_{\min}$, $x_{N+M} = x_{\max}$, and N is the number of collocation points. Note that collocation points are denoted by greek subscripts. We can now write a linear system of equations by evaluating (20) at these collocation points

$$f_\alpha = \sum_i B_{\alpha i} c^i, \quad (22)$$

where $f_\alpha \equiv f(x_\alpha)$, and $B_{\alpha i} \equiv B_i^M(x_\alpha)$. In order to solve for the expansion coefficients, the matrix \mathbf{B} needs to be inverted. However, as it stands, the matrix \mathbf{B} is not a

square matrix, since the total number of splines with a nonzero extension in the physical region is $N + M - 1$. In order to perform the inversion, we need to introduce additional linear equations which represent the boundary conditions imposed on $f(x)$ at the two boundary points, x_M and x_{M+N} . The essence of the lattice method is to eliminate the expansion coefficients c^i using this inverse matrix. The details of using the boundary conditions and inverting the resulting square matrix are discussed elsewhere [18]. Following the inversion, the coefficients are given by

$$c^i = \sum_{\alpha} [\mathbf{B}^{-1}]^{i\alpha} f_{\alpha}. \quad (23)$$

One can trivially show that all local functions will have a local representation in the finite dimensional collocation space

$$f(x) \longrightarrow f_{\alpha}. \quad (24)$$

The collocation representation of the operators can be obtained by considering the action of an operator \mathcal{O} onto a function $f(x)$

$$\mathcal{O}f(x) = \sum_i [\mathcal{O}B_i^M(x)]c^i. \quad (25)$$

If we evaluate the above expression at the collocation points x_{α} , we can write

$$[\mathcal{O}f]_{\alpha} = \sum_i [\mathcal{O}B]_{\alpha i} c^i. \quad (26)$$

Substituting from Eq. (23) for the coefficients c^i , we obtain

$$S = \int dt \sum_{\alpha\beta\gamma} \Delta V_{\alpha\beta\gamma} \left\{ \mathcal{H}(\alpha\beta\gamma) - \left[i\hbar \sum_{\mu} \psi_{\mu}^*(\alpha\beta\gamma) \frac{\partial \psi_{\mu}}{\partial t}(\alpha\beta\gamma) \right] \right\}, \quad (29)$$

where indices α, β , and γ denote the lattice points in three-dimensional space, and $\Delta V_{\alpha\beta\gamma}$ is the corresponding infinitesimal volume element. Due to the presence of derivative operators in the Hamiltonian, the explicit form of these expressions will depend nonlocally on the lattice indices. The general variation, which preserves the properties of the continuous variation, is given by

$$\frac{\delta \psi_{\mu}^*(\alpha\beta\gamma)}{\delta \psi_{\lambda}^*(\alpha'\beta'\gamma')} = \frac{1}{\Delta V_{\alpha\beta\gamma}} \delta_{\lambda\mu} \delta_{\alpha'\alpha} \delta_{\beta'\beta} \delta_{\gamma'\gamma}. \quad (30)$$

The details of the discrete variation for the finite-difference case are given in Refs. [5, 6]. Below we outline a procedure for using the spline collocation method for the numerical solution of HF and TDHF equations.

Since the detailed derivation of the representation of the TDHF equations involves many terms that are present in the energy functional, we will only illustrate a few terms. The three-dimensional expansion in terms of splines is a simple generalization of Eq. (20)

$$\begin{aligned} [\mathcal{O}f]_{\alpha} &= \sum_{i\beta} [\mathcal{O}B]_{\alpha i} [\mathbf{B}^{-1}]^{i\beta} f_{\beta} \\ &= \sum_{\beta} O_{\alpha}^{\beta} f_{\beta}, \end{aligned} \quad (27)$$

where we have defined the collocation space matrix representation of the operator \mathcal{O} by

$$O_{\alpha}^{\beta} = \sum_i [\mathcal{O}B]_{\alpha i} [\mathbf{B}^{-1}]^{i\beta}. \quad (28)$$

Notice that the construction of the collocation space operators can be performed once and for all at the beginning of a calculation, using only the given knot sequence and collocation points. Due to the presence of the inverse in Eq. (28), the matrix O is not sparse. In practice, the operator \mathcal{O} is chosen to be a differential operator such as d/dx or d^2/dx^2 . By a similar construction, it is also possible to obtain the appropriate integration weights on the collocation lattice [18].

B. HF Equations in collocation space

In order to obtain a set of lattice equations which preserve the conservation laws associated with the continuous equations, it is essential to develop a modified variational approach. This goal is achieved by performing a variation to the discretized form of a conserved quantity, i.e., total energy. Consequently, the resulting equations will preserve all of the conserved quantities on the lattice. For the TDHF equations, we consider a general discretized form of the action (static HF is obtained by using a trivial time-phase for the single-particle states)

$$\psi_{\lambda}(x, y, z) = \sum_{ijk} c_{\lambda}^{ijk} B_i(x) B_j(y) B_k(z). \quad (31)$$

The knots and collocation points for each coordinate can be different. With the appropriate definition of boundary conditions, all of the discretization techniques discussed in the previous section can be generalized to the three-dimensional space. The details of this procedure are given in Ref. [18].

As an example for a local term, let us consider a part of the t_0 contribution to the total energy

$$\begin{aligned} &\frac{t_0}{2} \left(1 + \frac{x_0}{2}\right) \int d^3r \rho^2 \\ &= \frac{t_0}{2} \left(1 + \frac{x_0}{2}\right) \sum_{\alpha\beta\gamma} w^{\alpha} w^{\beta} w^{\gamma} [\rho(\alpha\beta\gamma)]^2, \end{aligned} \quad (32)$$

where on the right-hand side we have written the discretized form on a collocation lattice with integration

TABLE II. A comparative study of HF results for ^{16}O . The force used is the BKN. We also include the direct and exchange parts of the Coulomb interaction and consider separate neutron and proton densities.

	Radial $N = 500$ $\Delta = 0.025$ fm	Spline, $M = 3$ $N = 22^3$ $\Delta = 0.9$ fm	Spline, $M = 5$ $N = 22^3$ $\Delta = 0.9$ fm	Spline, $M = 7$ $N = 22^3$ $\Delta = 0.9$ fm
E_{HF} (MeV)	-119.641	-113.849	-119.135	-119.674
E_K (MeV)	249.734	250.416	249.809	250.070
r_p (fm)	2.6263	2.6491	2.6284	2.6254
r_n (fm)	2.5970	2.6202	2.5993	2.5961
$E_s(n)$ (MeV)	-30.120	-30.181	-30.160	-30.148
$E_p(n)$ (MeV)	-16.949	-16.702	-16.954	-16.975
$E_s(p)$ (MeV)	-26.237	-26.351	-26.282	-26.265
$E_p(p)$ (MeV)	-13.361	-13.167	-13.372	-13.386

weights denoted by w . Here, α , β , and γ represent the collocation points in x , y , and z directions, respectively. In order to be able to perform the variation with respect to the single-particle states ψ_λ^* , we rewrite Eq. (32) explicitly

$$\frac{t_0}{2} \left(1 + \frac{x_0}{2}\right) \sum_{\alpha\beta\gamma} w^\alpha w^\beta w^\gamma \sum_{\mu\nu} \psi_\mu^* \psi_\mu \psi_\nu^* \psi_\nu. \quad (33)$$

Using Eq. (30) in the variation of Eq. (33), we obtain (after replacing the primed indices with unprimed ones) the contribution

$$t_0 \left(1 + \frac{x_0}{2}\right) \rho(\alpha\beta\gamma) \psi_\lambda(\alpha\beta\gamma), \quad (34)$$

where we have rewritten a summation as the total density. The same procedure can be carried out for the non-local terms in the energy density. A typical term is illustrated below

$$(\nabla\psi_\lambda^\pm)_{\alpha\beta\gamma} = \sum_{\alpha'} D_{\alpha'}^{\alpha'} \psi_\lambda^\pm(\alpha'\beta\gamma) \hat{\mathbf{i}} + \sum_{\beta'} D_{\beta'}^{\beta'} \psi_\lambda^\pm(\alpha\beta'\gamma) \hat{\mathbf{j}} + \sum_{\gamma'} D_{\gamma'}^{\gamma'} \psi_\lambda^\pm(\alpha\beta\gamma') \hat{\mathbf{k}},$$

where the matrices \mathbf{D} denote the first derivative matrices

in x , y , and z directions (they can be different although the notation does not make this obvious) calculated as described in the previous section. Finally, the HF equations can be written as matrix-vector equations on the collocation lattice

$$h\psi_\lambda^\pm \longrightarrow \mathbf{h} \cdot \psi_\lambda^\pm. \quad (35)$$

The essence of this construction is that the terms in the single-particle Hamiltonian \mathbf{h} are matrices in one coordinate and diagonal in others. Therefore, \mathbf{h} need not be stored as a full matrix, which allows the handling of very large systems directly in memory. The details of this procedure are discussed below.

C. Solution of the discrete HF equations

The solution of the HF Eqs. (35) is found by using the damped relaxation method described in Refs. [26, 4]

$$\chi_\lambda^{k+1} = \mathcal{O}[\chi_\lambda^k - x_0 \mathbf{D}(E_0)(\mathbf{h}^k - \epsilon_\lambda^k) \chi_\lambda^k], \quad (36)$$

where \mathcal{O} stands for Gram-Schmidt orthonormalization.

TABLE III. A comparative study of HF results for ^{16}O . The force used is the SkM*. We also include the direct and exchange parts of the Coulomb interaction and consider separate neutron and proton densities.

	Radial $N = 500$ $\Delta = 0.025$ fm	3D, $M = 3$ $N = 22^3$ $\Delta = 0.9$ fm	3D, $M = 5$ $N = 22^3$ $\Delta = 0.9$ fm	3D, $M = 7$ $N = 22^3$ $\Delta = 0.9$ fm	3D, $M = 9$ $N = 22^3$ $\Delta = 0.9$ fm
E_{HF} (MeV)	-127.73	-122.20	-127.18	-127.69	-127.73
r_{rms} (fm)	2.6822	2.7179	2.6872	2.6826	2.6821
$E_{s_{1/2}}(n)$ (MeV)	-33.307	-33.038	-33.305	-33.311	-33.308
$E_{p_{3/2}}(n)$ (MeV)	-19.882	-19.249	-19.814	-19.873	-19.880
$E_{p_{1/2}}(n)$ (MeV)	-13.551	-13.452	-13.515	-13.540	-13.545
$E_{s_{1/2}}(p)$ (MeV)	-29.739	-29.523	-29.741	-29.743	-29.740
$E_{p_{3/2}}(p)$ (MeV)	-16.477	-15.908	-16.415	-16.468	-16.474
$E_{p_{1/2}}(p)$ (MeV)	-10.270	-10.226	-10.242	-10.260	-10.265

TABLE IV. A comparative study of HF results for ^{16}O . The force used is the SkM*.

	Radial $N = 500$ $\Delta = 0.025$ fm	3D, $M = 7$ $N = 12^3$ $\Delta = 1.667$ fm	3D, $M = 7$ $N = 22^3$ $\Delta = 0.909$ fm	3D, $M = 7$ $N = 33^3$ $\Delta = 0.606$ fm
E_{HF} (MeV)	-127.73	-127.36	-127.69	-127.73
r_{rms} (fm)	2.6822	2.6872	2.6826	2.6822
$E_{s_{1/2}}(n)$ (MeV)	-33.307	-33.119	-33.311	-33.307
$E_{p_{3/2}}(n)$ (MeV)	-19.882	-20.131	-19.873	-19.882
$E_{p_{1/2}}(n)$ (MeV)	-13.551	-13.551	-13.540	-13.551
$E_{s_{1/2}}(p)$ (MeV)	-29.739	-29.584	-29.743	-29.739
$E_{p_{3/2}}(p)$ (MeV)	-16.477	-16.718	-16.468	-16.475
$E_{p_{1/2}}(p)$ (MeV)	-10.270	-10.284	-10.260	-10.269

The damping operator \mathbf{D} is chosen to be [26, 4]

$$\mathbf{D}(E_0) = \left[1 + \frac{\mathbf{T}}{E_0} \right]^{-1} \\ \approx \left[1 + \frac{\mathbf{T}_x}{E_0} \right]^{-1} \left[1 + \frac{\mathbf{T}_y}{E_0} \right]^{-1} \left[1 + \frac{\mathbf{T}_z}{E_0} \right]^{-1},$$

where \mathbf{T} denotes the kinetic-energy operator. In practical calculations we have used the damping scale value $x_0 = 0.05$ and the energy cutoff $E_0 = 20.0$. As a convergence criteria we have required the fluctuations in energy

$$\Delta E^2 \equiv \sqrt{\langle H^2 \rangle - \langle H \rangle^2} \quad (37)$$

to be less than 10^{-6} . This is a more stringent condition than the simple energy difference between two iterations, which is about 10^{-13} when the fluctuation accuracy is satisfied.

The calculation of the HF Hamiltonian also requires the evaluation of Yukawa and direct Coulomb contributions given by Eqs. (18) and (19). The evaluation of the three-dimensional integrals is very costly; instead, we solve the corresponding differential equations

$$\left(\nabla^2 - \frac{1}{a^2} \right) W_Y(\mathbf{r}) = -4\pi a \rho_q(\mathbf{r}), \\ \nabla^2 U_C(\mathbf{r}) = -4\pi e^2 \rho_p(\mathbf{r}).$$

Details of solving the Helmholtz and Poisson equations using the splines are given in Ref. [18].

IV. RESULTS

In Table II we have tabulated the results obtained from the solution of the three-dimensional HF equations to-

gether with the solution of the radial Schrödinger equation for the spherical ^{16}O nucleus, using the Bonche-Koonin-Negele (BKN) force [27]. Three-dimensional calculations result in a spherical nucleus with a quadrupole moment on the order of 10^{-13} fm². We have used 22 points in x -, y -, and z - directions in interval $(-10, +10)$ fm. Radial calculations had converged to two significant digits. As we see from Table II, an increase in the spline order M leads to a significant improvement in all quantities. The error in binding energy for $M = 7$ is 0.03%. The energies were calculated using the Koopman's formula with corrections for the density-dependent three-body term and the Coulomb exchange. We also correct the energy for the center of mass motion using the approximation $E_{\text{c.m.}} = \sum_i p_i^2 / 2Am$. The three-dimensional calculations involve 16 single-particle states each with a spin-up and a spin-down component. Due to the absence of the spin-orbit interaction in the BKN force, the 6 p states for neutrons and protons are degenerate in energy. In Table III we repeat the ^{16}O calculations using the SkM* force. The table shows the same level of convergence for this force even though the SkM* includes the complicated spin-orbit interaction. In this case the numerical computation of the parity and the third component of the total angular momentum using equations

$$\pi_s = \int d^3r \phi_\lambda^*(\mathbf{r}) \phi_\lambda(-\mathbf{r}), \\ J_z = \langle \phi_\lambda | l_z + \sigma_z | \phi_\lambda \rangle$$

are within 1 part in 10^4 of the exact spherical value. We also note that the $1p$ splitting for the ^{16}O is accurately reproduced as 6.15 MeV. Each HF calculation for ^{16}O on a $(22)^3$ lattice consumed 15 min on a Cray-2 su-

TABLE V. A comparison of radial HF calculations with three-dimensional spline results for the ^{40}Ca nucleus. The force used is the SkM* interaction. We have used a spline order $M = 7$ with a $(24)^3$ lattice and 0.9 fm spacing.

	E_{HF} (MeV)	r_{rms} (fm)	Q_{20}
Radial	-341.11	3.4016	0
3D	-341.00	3.4023	2×10^{-4}

TABLE VI. A comparison of radial HF single-particle energies with three-dimensional spline results for the ^{40}Ca nucleus. The force used is the SkM* interaction. We have used a spline order $M = 7$ with a $(24)^3$ lattice and 0.9 fm spacing.

		$1S_{1/2}$	$1P_{3/2}$	$1P_{1/2}$	$1D_{5/2}$	$2S_{1/2}$	$1D_{3/2}$
n	Radial	-43.813	-32.671	-28.563	-21.373	-16.743	-14.323
	3D	-43.815	-32.668	-28.563	-21.364	-16.735	-14.316
p	Radial	-36.326	-25.394	-21.379	-14.334	-9.744	-7.477
	3D	-36.330	-25.394	-21.381	-14.328	-9.739	-7.473

percomputer. The computer time for heavier systems is somewhat linearly proportional to their mass number. In Table IV we have repeated these calculations for a fixed order of splines, $M = 7$. The number of lattice points increases from $(12)^3$ to $(33)^3$ showing the clear convergence of all quantities as a function of the number of collocation points. From these results, one may conclude that with $M = 9$ a lattice dimension between $(12)^3$ and $(22)^3$ is generally adequate.

Tables V and VI show similar calculations for the ^{40}Ca nucleus using the SkM* force. The calculations used a spline of order $M = 7$ and a $(24)^3$ lattice with 0.9 fm lattice spacing in each direction. We observe from Table V that the numerically computed value of the quadrupole moment is 2×10^{-4} which could be improved by demanding a stricter convergence criteria. In Table VI we compare the single-particle energies between the radial and three-dimensional calculations. We observe that the results are strikingly accurate. These results could further be improved by performing calculations with $M = 9$ which require the same amount of computer time due to the use of nonsparse derivative matrices. These calculations involve 40 single-particle states each having a spin-up and a spin-down component represented on the three-dimensional Cartesian lattice.

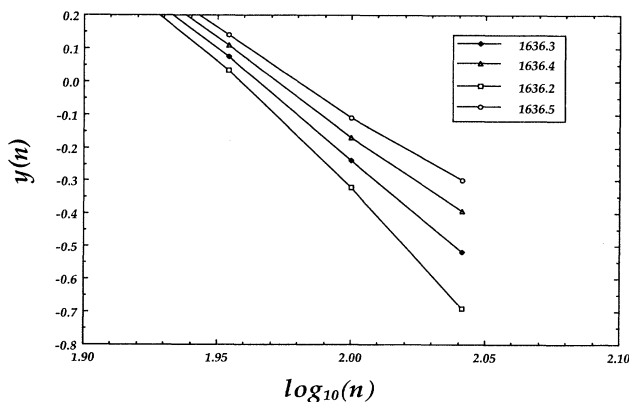


FIG. 1. A plot demonstrating the search for the extrapolated value of the HF energy. Notice that the curve with $f_\infty = 1636.4$ MeV is quite close to being linear.

For larger systems, such as the ^{208}Pb , which involves 208 single-particle states each with spin-up and spin-down components, the calculations on a Cray-2 require a modest amount of computer time. We have performed one such calculation for the ^{208}Pb system using $M = 9$ and a $(22)^3$ lattice. The calculations were stopped after 110 iterations which took 10 CPU hours on the Cray-2. At the last iteration the binding energy was -1636.0 MeV, which should be compared with the exact spherical value of -1636.4 MeV. The convergence of other observables were commensurate with this result. The rate of convergence for large systems is relatively slow towards the end of a calculation when the results have converged to better than one percent in accuracy. However, there exists powerful extrapolation methods for dealing with such slow convergences [32]. One can show that the asymptotic expansion for the binding energy and the nuclear radius have the form

$$\lim_{n \rightarrow \infty} f(n) \rightarrow f_\infty + \frac{A}{n^b}, \quad (38)$$

where A and b are constants and f_∞ denotes the con-

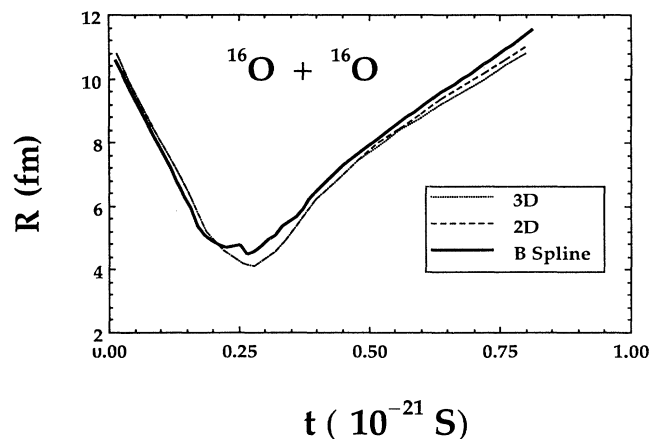


FIG. 2. Comparison of three-dimensional, spline TDHF calculations (solid line) with symmetric three-dimensional results (dotted line) and axially symmetric calculations (dot-dashed line).

verged result. For finite data sets this is actually non-linear in f_∞ and requires a search for f_∞ . Rewriting Eq. (38) as

$$f(n) - f_\infty = \frac{A}{n^b} \equiv 10^{y(n)}, \quad (39)$$

we obtain

$$y(n) = \log_{10} A - b \log_{10}(n). \quad (40)$$

For every guess of f_∞ we find constants A and b which produce the most linear $y(n)$ vs $\log_{10}(n)$ curve. A typical search is graphed in Fig. 1. We note that the most linear curve corresponds to 1636.4 MeV, same as the radial HF result.

At this time we have also completed one TDHF calculation for the $^{16}\text{O}+^{16}\text{O}$ system at $E_{\text{lab}} = 64$ MeV using the BKN force with an impact parameter $b = 0.0$ fm. We have used a time step of $\Delta t = 0.4$ fm/c and followed the reaction for 850 time steps. These numbers are commensurate with the few restricted three-dimensional calculations available in the literature [28–31]. At the end of the calculation the discrepancy in energy was 32 keV out of the total energy of 193 MeV, an error of 0.02%. During the collision the overall normalization was conserved to better than 1 part in 10^8 . In Fig. 2 we show the distance between the two nuclei calculated using the spline method in unrestricted space (solid line) for $E_{\text{lab}} = 64$ MeV and for a head-on (zero impact parameter) collision. The other curves show the symmetric three-dimensional calculations of Ref. [28] (dotted line), and the cylindrical calculation (dot-dashed line). The reduction of the TDHF equations to axial symmetry is exact for head-on collisions. These calculations provide a test of our results for very low-energy collisions and for using forces that are fitted to reproduce the data. The generaliza-

tion to higher energies, interactions, and nonzero impact parameters are being presently calculated.

V. DISCUSSION

We have performed three-dimensional HF and TDHF calculations with no simplifying assumptions. The use of the spline collocation method results in an unprecedented accuracy for relatively coarse meshes. The evolution of nuclear HF and TDHF calculations have closely paralleled the advances made in computer technology. With these new numerical methods and the technology available today it is possible to perform static HF calculations with accuracies comparable to more phenomenological models. In the near future we will incorporate constraints into the HF program which will enable us to perform energy-surface calculations for heavier systems. Similarly, unrestricted dynamical calculations will help us correctly address the questions about the amount of mean-field dissipation present in heavy-ion collisions. But, perhaps more importantly, the development of such numerical technologies and programs will lead to spin-offs for addressing many other problems in physics.

ACKNOWLEDGMENTS

This research was sponsored in part by the U.S. Department of Energy under Contract No. DE-AC05-84OR21400 with Martin Marietta Energy Systems, Inc. and under Contract No. DE-FG05-87ER40376 with Vanderbilt University. The numerical calculations were partially carried out on CRAY-2 supercomputers at the National Center for Supercomputing Applications, Illinois, and at the National Energy Research Supercomputing Center, Livermore.

-
- [1] K. T. R. Davies, K. R. S. Devi, S. E. Koonin, and M. R. Strayer, in *Treatise on Heavy Ion Science*, edited by D. A. Bromley (Plenum, New York, 1985), Vol.3, p. 3.
 - [2] J. W. Negele, *Rev. Mod. Phys.* **54**, 913 (1982).
 - [3] A. S. Umar and M. R. Strayer, in *Time-Dependent Methods for Quantum Dynamics*, a special thematic issue, *Comput. Phys. Commun.* **63**, 179 (1991).
 - [4] A. S. Umar, M. R. Strayer, R. Y. Cusson, P.-G. Reinhard, and D. A. Bromley, *Phys. Rev. C* **32**, 172 (1985).
 - [5] A. S. Umar, M. R. Strayer, P. -G. Reinhard, K. T. R. Davies, and S. -J. Lee, *Phys. Rev. C* **40**, 706 (1989).
 - [6] K. T. R. Davies and S. E. Koonin, *Phys. Rev. C* **23**, 2042 (1981).
 - [7] P. Hoodbhoy and J. W. Negele, *Nucl. Phys.* **A288**, 23 (1977).
 - [8] S. E. Koonin, K. T. R. Davies, V. Maruhn-Rezwani, H. Feldmeier, S. J. Krieger, and J. W. Negele, *Phys. Rev. C* **15**, 1359 (1977).
 - [9] P. -G. Reinhard, A. S. Umar, K. T. R. Davies, M. R. Strayer, and S. -J. Lee, *Phys. Rev. C* **37**, 1026 (1988).
 - [10] S. -J. Lee, A. S. Umar, K. T. R. Davies, M. R. Strayer, and P. -G. Reinhard, *Phys. Lett. B* **196**, 419 (1987).
 - [11] A. S. Umar, M. R. Strayer, and P.-G. Reinhard, *Phys. Rev. Lett.* **56**, 2793 (1986).
 - [12] J. Bartel, P. Quentin, M. Brack, C. Guet, and H. B. Hakansson, *Nucl. Phys.* **A386**, 79 (1982).
 - [13] P. Bonche, H. Flocard, P. H. Heenen, S. J. Krieger, and M. S. Weiss, *Nucl. Phys.* **A443**, 39 (1985).
 - [14] P. Bonche, H. Flocard, and P. H. Heenen, *Nucl. Phys.* **A467**, 115 (1987).
 - [15] P. Bonche, S. J. Krieger, P. Quentin, M. S. Weiss, J. Meyer, M. Meyer, N. Redon, H. Flocard, and P. H. Heenen, *Nucl. Phys.* **A500**, 308 (1989).
 - [16] J. F. Berger, J. D. Anderson, P. Bonche, and M. S. Weiss, *Phys. Rev. C* **41**, R2483 (1990).
 - [17] P. Bonche, H. Flocard, and P. H. Heenen, *Nucl. Phys.* **A523**, 300 (1991).
 - [18] A. S. Umar, J. Wu, M. R. Strayer, and C. Bottcher, *J. Comput. Phys.* **93**, 426 (1991).
 - [19] A. S. Umar, in *Proceedings of Summer School of Computational Atomic and Nuclear Physics*, edited by C. Bottcher and M. R. Strayer (World Scientific, New York, 1990), p. 377.
 - [20] A. K. Kerman and S. E. Koonin, *Ann. Phys. (N.Y.)* **100**, 332 (1976).
 - [21] D. Vautherin and D. M. Brink, *Phys. Rev. C* **5**, 626

- (1972).
- [22] Y. M. Engel, D. M. Brink, K. Goeke, S. J. Krieger, and D. Vautherin, Nucl. Phys. **A249**, 215 (1975).
- [23] P. Quentin and H. Flocard, Annu. Rev. Nucl. Sci. **28**, 523 (1978).
- [24] M. J. Giannoni and P. Quentin, Phys. Rev. C **21**, 2076 (1980).
- [25] C. De Boor, *Practical Guide to Splines* (Springer-Verlag, New York, 1978).
- [26] C. Bottcher, M. R. Strayer, A. S. Umar, and P. -G. Reinhard, Phys. Rev. A **40**, 4182 (1989).
- [27] P. Bonche, S. E. Koonin, and J. W. Negele, Phys. Rev. C **13**, 1226 (1976).
- [28] H. Flocard, S. E. Koonin, and M. S. Weiss, Phys. Rev. C **17**, 1682 (1978).
- [29] P. Bonche, B. Grammaticos, and S. E. Koonin, Phys. Rev. C **17**, 1700 (1978).
- [30] K. T. R. Davies, H. T. Feldmeier, H. Flocard, and M. S. Weiss, Phys. Rev. C **18**, 2631 (1978).
- [31] K. R. Sandhya Devi, M. R. Strayer, J. M. Irvine, and K. T. R. Davies, Phys. Rev. C **23**, 1064 (1981).
- [32] L. M. Delves, in *Advances in Nuclear Physics*, edited by M. Baranger and E. Vogt (Plenum, New York, 1973), p. 1.